ISSN 0021-8944, Journal of Applied Mechanics and Technical Physics, 2019, Vol. 60, No. 2, pp. 365–376. © Pleiades Publishing, Ltd., 2019.
Original Russian Text © A.A. Chesnokov, V.Yu. Liapidevskii.

EVOLUTION OF THE HORIZONTAL MIXING LAYER IN SHALLOW WATER

A. A. Chesnokov and V. Yu. Liapidevskii

UDC 532.517+532.591

Abstract: Horizontal shear motion of a homogeneous fluid in an open channel is considered in the approximation of the shallow water theory. The main attention is paid to studying the mixing process induced by the development of the Kelvin–Helmholtz instability and by the action of bottom friction. Based on a three-layer flow pattern, an averaged one-dimensional model of formation and evolution of the horizontal mixing layer is derived with allowance for friction. Steady solutions of the equations of motion are constructed, and the problem of the mixing layer structure is solved. The bottom friction produces a stabilizing effect and reduces the growth of the mixing layer. Verification of the proposed one-dimensional model is performed through comparisons with available experimental data and with the numerical solution of the two-dimensional equations of the shallow water theory.

Keywords: shallow water equations, horizontal shear flow, mixing layer, effect of friction.

DOI: 10.1134/S0021894419020172

INTRODUCTION

The interest in studying shear flows and horizontal mixing in a thin layer of the fluid is inspired by numerous geophysical and engineering applications [1, 2]. Examples of such flows in nature are mixing layers and jets formed in regions of confluence of rivers and river mouths, and also wake vortices formed in the flow around islands and other obstacles. A typical ratio of the vertical and horizontal scales for flows of such a class is usually very small, and the development of shear instability can be described within the framework of the shallow water theory [3, 4]. The character of the flow and the evolution of mixing are determined by interaction of horizontal vortices arising at the nonlinear stage of the development of the Kelvin–Helmholtz instability and by bottom friction caused by a small depth of the reservoir.

The experimental study of horizontal mixing layers [5–7] shows that the effect of bottom friction is insignificant in fluid layers of a sufficiently large thickness and also at the initial stage of instability development in thinner layers. As the thickness of the layers moving with different velocities decreases, the increase in the intermediate mixing layer width is terminated at a certain distance from the confluence region. Determination of the flow parameters at which the entrainment processes are terminated was the main goal of the experiments described in [5–7]. Mathematical models of the horizontal mixing layer development based on the averaged equations of the shallow water theory were presented and verified in [8–10]. Results of numerical simulations of horizontal mixing in the case of confluence of flows moving with different velocities were reported in [11, 12].

Lavrentyev Institute of Hydrodynamics, Siberian Branch, Russian Academy of Sciences, Novosibirsk, 630090 Russia. Novosibirsk State University, Novosibirsk, 630090 Russia; chesnokov@hydro.nsc.ru; liapid@hydro.nsc.ru.
Translated from Prikladnaya Mekhanika i Tekhnicheskaya Fizika, 2019, Vol. 60, No. 2, pp. 207–219, March–April, 2019 Original article submitted August 29, 2018; revision submitted August 29, 2018; accepted for publication September 3, 2018.

An integrodifferential model of horizontal shear motion of the fluid in an open channel, which is equivalent to the Benny equations of vortical shallow water [13], was derived and studied in [14, 15]. Subsequent generalization and complication of this model were caused by the necessity of describing the nonlinear stage of the development of the Kelvin–Helmholtz instability and the formation of a turbulent mixing layer. The method of constructing one-dimensional models of propagation of long-wave perturbations in the shear flow with allowance for turbulent mixing is based on using the multilayer shallow water theory [16]. This approach was applied in [17] for deriving a model of a subsurface turbulent mixing layer in plane-parallel flows and describing the horizontal mixing in fluid layers of a sufficiently large thickness in open channels [18]. It should be noted that the development of models of layered motion of the fluid was significantly affected by the famous paper of Ovsyannikov dealing with models of two-layer shallow water [19].

The goals of the present study are to derive, analyze, and verify one-dimensional equations of three-layer flows of a homogeneous fluid with a free surface with allowance for bottom friction and mixing in the intermediate layer. The main attention is paid to studying the processes of attenuation of horizontal mixing due to friction. Steady solutions of the problem of mixing layer evolution in an open channel are obtained. The model is verified through comparisons with available experimental data on flow parameters in the mixing layer and with results of numerical simulations based on two-dimensional equations of the shallow water theory.

1. EQUATIONS OF MOTION

A spatial flow of a thin layer of a homogeneous fluid with a free boundary in the gravity field above a smooth bottom is described by the equations of the shallow water theory:

$$\begin{gathered} h_t + (Uh)_x + (Vh)_y = 0, \\ (Uh)_t + (U^2h + gh^2/2)_x + (UVh)_y = -c_f U\sqrt{U^2+V^2}, \\ (Vh)_t + (UVh)_x + (V^2h + gh^2/2)_y = -c_f V\sqrt{U^2+V^2}. \end{gathered} \tag{1}$$

Here x and y are the spatial variables, t is the time, U and V are the velocity vector components, h is the fluid layer thickness, g is the acceleration due to gravity, and c_f is the bottom friction coefficient.

Let us consider the flow of an ideal fluid in an extended open channel with side walls $y = Y_1(t,x)$ and $y = Y_2(t,x)$ and smooth bottom ($z = 0$). Assuming that the fluid motion occurs predominantly in the Ox direction, we apply scaling in Eqs. (1)

$$t \to \varepsilon^{-1}t, \quad x \to \varepsilon^{-1}x, \quad V \to \varepsilon V, \quad c_f \to \varepsilon c_f$$

and omit terms of the order of ε^2 ($\varepsilon \ll 1$ is the ratio of the characteristic transverse scale of the channel H_0 to the longitudinal scale L_0). As a result, we obtain the equations of horizontal shear motion of a thin fluid layer in a long open channel

$$\begin{gathered} h_t + (Uh)_x + (Vh)_y = 0, \qquad h_y = 0, \\ (Uh)_t + (U^2h + gh^2/2)_x + (UVh)_y = -c_f U|U| \end{gathered} \tag{2}$$

with the boundary conditions on the side walls

$$Y_{it} + UY_{ix} - V\Big|_{y=Y_i} = 0 \qquad (i = 1, 2). \tag{3}$$

The equations of motion (2), (3) in the absence of bottom friction ($c_f = 0$) were derived and studied in [14, 15].

System (2) yields the energy balance equation

$$E_t + ((E+P)U)_x + ((E+P)V)_y = -c_f|U|^3, \tag{4}$$

where $E = (U^2 + gh)h/2$ and $P = gh^2/2$. It should be also noted that the potential vorticity $\Omega = U_y/h$ satisfies the equation

$$\Omega_t + U\Omega_x + V\Omega_y = -2c_f|U|\Omega/h \tag{5}$$

and conserves along the trajectories in the absence of bottom friction.

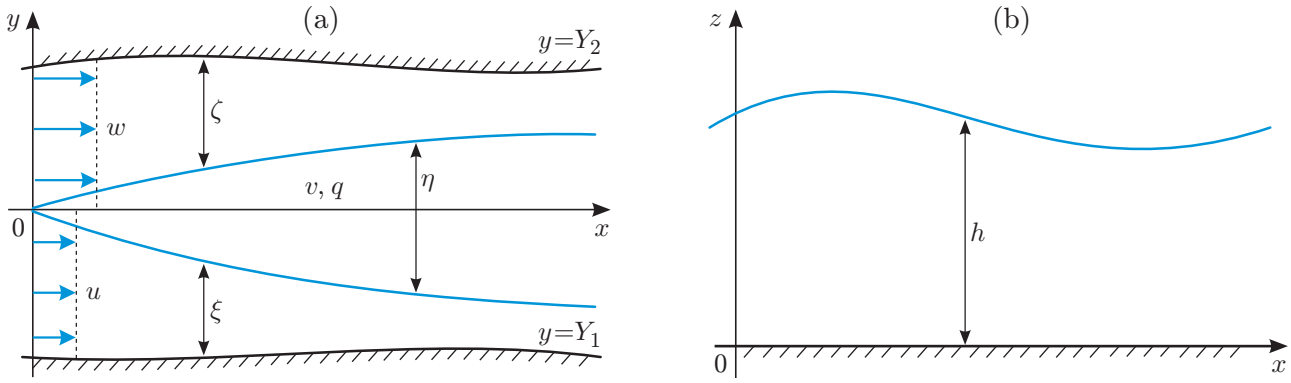

Fig. 1. Horizontal shear flow of a homogeneous fluid in an open channel: (a) top view; (b) side view.

1.1. Derivation of the Three-Layer Flow Model

The averaged model proposed below is meant to describe the horizontal mixing layer formed in an open channel between two almost potential layers of widths $\xi(t,x)$ and $\zeta(t,x)$. The flow pattern is schematically shown in Fig. 1. We assume that the velocity profile $U(t,x,y)$ satisfies the condition

$$U_y = \begin{cases} O(\varepsilon^\beta), & y \in (Y_1, Y_1+\xi) \cup (Y_2-\zeta, Y_2), \\ O(\varepsilon^\gamma), & y \in (Y_1+\xi, Y_2-\zeta) \end{cases} \tag{6}$$

with the parameters $\beta \in (1,2]$ and $\gamma \in (0,1)$. The case with $\beta = 2$ corresponds to a potential flow in interlayers of widths $\xi(t,x)$ and $\zeta(t,x)$.

To describe a three-layer flow, we introduce the averaged velocities in the layers and the root-mean-square deviation (shear velocity q) in the intermediate layer:

$$u = \frac{1}{\xi}\int\limits_{Y_1}^{Y_1+\xi} U\,dy, \quad w = \frac{1}{\zeta}\int\limits_{Y_2-\zeta}^{Y_2} U\,dy, \quad v = \frac{1}{\eta}\int\limits_{Y_1+\xi}^{Y_2-\zeta} U\,dy, \quad q^2 = \frac{1}{\eta}\int\limits_{Y_1+\xi}^{Y_2-\zeta} (U-v)^2\,dy. \tag{7}$$

To simplify further transformations, we assume that $U(t,x,y) \geq 0$; hence, the averaged velocities in the layers u, v, and w are non-negative.

The process of fluid entrainment from almost potential interlayers to the mixing layer is taken into account by the kinematic conditions on the internal interfaces

$$\begin{gathered} (Y_1+\xi)_t + U(Y_1+\xi)_x - V\Big|_{y=Y_1+\xi} = -M, \\ (Y_2-\zeta)_t + U(Y_2-\zeta)_x - V\Big|_{y=Y_2-\zeta} = M. \end{gathered} \tag{8}$$

The process of fluid entrainment from the external layers to the interlayer is assumed to be symmetric. Following [16, 18], we assume that the velocity of fluid entrainment into the vortex interlayer is proportional to the velocity of "large eddies" generated in the vicinity of the interface between the layers due to shear instability. Therefore, we further assume that

$$M = \sigma q.$$

According to [16], the proportionality coefficient σ is approximately equal to 0.15.

In averaging the equations of motion (2) and (4) over the channel width, there arises the necessity of approximate calculation of integrals of U^2 and U^3 with respect to the variable y. The following estimates are valid for almost potential layers:

$$\int\limits_{Y_1}^{Y_1+\xi} U^2\,dy = \xi u^2 + O(\varepsilon^{2\beta}), \qquad \int\limits_{Y_2-\zeta}^{Y_2} U^2\,dy = \zeta w^2 + O(\varepsilon^{2\beta}) \qquad (1 < \beta \leq 2).$$

As terms of the order of ε^2 are ignored in deriving model (2), the velocity U is replaced in the course of averaging the equations of motion in the weakly shear flow region by the corresponding averaged values of u and w determined by Eqs. (7).

Using the obvious identity $U = v + (U - v)$, we calculate the integrals in the intermediate mixing layer:

$$\int\limits_{Y_1+\xi}^{Y_2-\zeta} U^2\,dy = (v^2+q^2)\eta, \qquad \int\limits_{Y_1+\xi}^{Y_2-\zeta} U^3\,dy = (v^2+3q^2)v\eta + P_3, \qquad P_3 = \int\limits_{Y_1+\xi}^{Y_2-\zeta} (U-v)^3\,dy\,. \tag{9}$$

By virtue of the estimates that follow from condition (6), we have $P_3 = O(\varepsilon^{3\gamma}) \ll \eta v q^2 = O(\varepsilon^{2\gamma})$, $0 < \gamma < 1$. Therefore, the value of P_3 is small as compared to other terms and can be omitted [20]. In the absence of bottom friction ($c_f = 0$), the potential vorticity $\Omega = U_y/h$ remains unchanged along the trajectories; therefore, for obtaining the estimates presented above, it is sufficient to satisfy condition (6) at the initial time. These estimates are also valid at $c_f > 0$ because the right side of Eq. (5) is proportional to the potential vorticity Ω with a certain negative multiplier. As a result of averaging the energy equation (4), we obtain a closing relation for the variable q, which characterizes the spatial inhomogeneity of the flow in the mixing layer.

With allowance for the adopted assumptions, the three-layer model of evolution of the horizontal mixing layer has the form

$$(\xi h)_t + (u\xi h)_x = -\sigma q h, \qquad (\eta h)_t + (v\eta h)_x = 2\sigma q h, \qquad (\zeta h)_t + (w\zeta h)_x = -\sigma q h,$$

$$u_t + (u^2/2 + gh)_x = -c_f u^2/h, \qquad w_t + (w^2/2 + gh)_x = -c_f w^2/h,$$

$$Q_t + \Big(u^2\xi h + (v^2+q^2)\eta h + w^2\zeta h + gh^2 Y/2\Big)_x = gh^2 Y_x/2 - c_f(u^2\xi + (v^2+q^2)\eta + w^2\zeta), \tag{10}$$

$$\Big(u^2\xi h + (v^2+q^2)\eta h + w^2\zeta h + gh^2 Y\Big)_t + \Big(u^3\xi h + (v^2+3q^2)v\eta h + w^3\zeta h + 2gQh\Big)_x$$

$$= -gh^2 Y_t - \varkappa\sigma h q^3 - 2c_f(u^3\xi + (v^2+3q^2)v\eta + w^3\zeta).$$

Here $Y = \xi+\eta+\zeta$ is a specified width of the channel, $Q = (u\xi+v\eta+w\zeta)h$ is the fluid flow rate, and the non-negative constants c_f, σ, and $\varkappa$ are the empirical parameters characterizing the bottom friction, mass transfer, and energy dissipation. Equations (10) form a closed system for determining the fluid layer thickness h, transverse sizes of the potential (ξ, ζ) and turbulent ($\eta = Y - \xi - \zeta$) layers, fluid velocities u, w, and v in these layers, and shear velocity q in the mixing layer.

The derivation of model (10) is based on averaging Eqs. (2) and (4) over the channel width with allowance for assumption (6) and boundary conditions (3) and (8). Integrating the first equation of system (2) with respect to the variable y in each layer with the use of the boundary conditions, we obtain the first three equations of system (10). It should be noted that the sum of these three equations is the mass conservation law $(Yh)_t + Q_x = 0$. After averaging the last equation of system (2) and the energy equation (4) over the width of one of the weakly shear layers, we have

$$(u\xi h)_t + (u^2\xi h)_x + g\xi h h_x + c_f\xi u^2 + \sigma q h U\Big|_{y=Y_1+\xi} = 0,$$

$$(u^2\xi h + gh^2\xi)_t + (u^3\xi h + 2gh^2 u\xi)_x + gh^2\xi_t + 2c_f\xi u^3 + \sigma q h\Big(U^2\Big|_{y=Y_1+\xi} + 2gh\Big) = 0. \tag{11}$$

With the use of averaging over another weakly shear layer, one can obtain the same equations with accuracy to the replacement of u, ξ, and $U\Big|_{y=Y_1+\xi}$ by w, ζ, and $U\Big|_{y=Y_2-\zeta}$, respectively. Following [21], for determining the velocity U on the internal boundaries of the layer, we use the condition of compatibility of the averaged equations of mass, momentum, and energy balance in almost potential layers. Direct calculations show that the first equation in system (10), equations (11), and also similar equations for the second weakly shear layer are compatible only if the following conditions are satisfied:

$$U\Big|_{y=Y_1+\xi} = u, \qquad U\Big|_{y=Y_2-\zeta} = w. \tag{12}$$

With allowance for Eqs. (12), the momentum equations for almost potential layers acquire the form of the fourth and fifth equations of system (10). After averaging the momentum equation in (2) over the entire channel width, we obtain the last-but-one equation of system (10). The last equation of system (10) (in the case with $\varkappa = 0$) is derived by means of averaging the energy balance equation (4). In modeling real flows, it is reasonable to take into account the energy dissipation; therefore, the right side of the last equation of system (10) is supplemented with a term that contains an empirical parameter $\varkappa$. According to [16], the value of $\varkappa$ is located in the interval from 2 to 6.

At $c_f = 0$, the equations of system (10) coincide with the equations of motion derived in [18] under more severe conditions for the velocity profile U [it was assumed that $U_y = 0$ at $y \in (Y_1, Y_1 + \xi) \cup (Y_2 - \zeta, Y_2)$].

1.2. Two-Layer and One-Layer Models

If one or two weakly shear layers are absent, system (10) is appreciably simplified. Let $\zeta = 0$ and $w = 0$, which corresponds to the two-layer flow model and to the formation of a turbulent jet. The equations of motion take the form

$$\begin{gathered}(\xi h)_t + (u\xi h)_x = -\sigma q h, \quad (\eta h)_t + (v\eta h)_x = \sigma q h, \quad u_t + (u^2/2 + gh)_x = -c_f u^2/h,\\ Q_t + \Big(u^2\xi h + (v^2+q^2)\eta h + gh^2 Y/2\Big)_x = gh^2 Y_x/2 - c_f(u^2\xi + (v^2+q^2)\eta),\\ \Big(u^2\xi h + (v^2+q^2)\eta h + gh^2 Y\Big)_t + \Big(u^3\xi h + (v^2+3q^2)v\eta h + 2gQh\Big)_x\\ = -gh^2 Y_t - \varkappa\sigma h q^3 - 2c_f(u^3\xi + (v^2+3q^2)v\eta).\end{gathered} \tag{13}$$

In the case of a one-layer flow, we additionally assume that $\xi = 0$ and $u = 0$. As a result, model (13) reduces to the following system of equations:

$$\begin{gathered}(Yh)_t + (vYh)_x = 0, \quad (vYh)_t + \Big((v^2+q^2)Yh + gYh^2/2\Big)_x = gh^2 Y_x/2 - c_f Y(v^2+q^2),\\ \Big((v^2+q^2)Yh + gYh^2\Big)_t + \Big((v^2+3q^2)vYh + 2gvYh^2\Big)_x\\ = -gh^2 Y_t - \varkappa\sigma h q^3 - 2c_f vY(v^2+3q^2).\end{gathered} \tag{14}$$

For a constant-width channel ($Y = \text{const}$), the equations of system (14) reduce to the gas-dynamic equations of the vortical shallow water model [20].

1.3. Differential Corollaries

It makes sense to derive some corollaries for the further analysis of the equations of motion and subsequent calculations. By virtue of any system of equations [(10), (13), or (14)], the mean flow velocity v in the vortical interlayer and the variable q satisfy the equations

$$v_t + vv_x + 2qq_x + \frac{q^2}{\eta}\,\eta_x + \Big(g + \frac{q^2}{h}\Big)h_x = f_1, \qquad q_t + (vq)_x = f_2. \tag{15}$$

For the three-layer flow [model (10)], the right sides of Eqs. (15) have the form

$$f_1 = \frac{\sigma q}{\eta}\,(u - 2v + w) - \frac{c_f}{h}\,(v^2+q^2), \quad f_2 = \frac{\sigma}{2\eta}\Big((u-v)^2 + (w-v)^2 - (2+\varkappa)q^2\Big) - \frac{2c_f}{h}\,vq.$$

For the two-layer flow [model (13)], the functions f_i in Eqs. (15) are defined as

$$f_1 = \frac{\sigma q}{\eta}\,(u - v) - \frac{c_f}{h}\,(v^2+q^2), \qquad f_2 = \frac{\sigma}{2\eta}\Big((u-v)^2 - (1+\varkappa)q^2\Big) - \frac{2c_f}{h}\,vq.$$

The corollary of the system for the one-layer flow (14) is Eqs. (15) (where it should be assumed that $\eta = Y$) with the right sides

$$f_1 = -\frac{c_f}{h}\,(v^2+q^2), \qquad f_2 = -\frac{\sigma\varkappa q^2}{2Y} - \frac{2c_f}{h}\,vq.$$

Using the differential corollaries (15), one can easily demonstrate that the equations for the one-layer flow (14) are hyperbolic (the propagation velocity of the characteristics is $dx/dt = v \pm \sqrt{gh + 3q^2}$). As was shown in [18], the two-layer and three-layer models (13) and (10) are not hyperbolic in the general case, but they always have at least three real characteristics (one contact characteristic $dx/dt = v$ and two acoustic characteristics). The existence of real characteristics allows one to use standard numerical methods developed for solving hyperbolic equations.

2. STATIONARY SOLUTIONS

To solve the problem of the mixing layer structure in a constant-section channel, it is sufficient to consider stationary flows.

2.1. Horizontal Mixing Layer

Stationary fluid flows in the three-layer model (10) with allowance for Eqs. (15) are determined by solving the system of ordinary differential equations

$$(u\xi h)' = -\sigma q h, \qquad (v\eta h)' = 2\sigma q h, \qquad (w\zeta h)' = -\sigma q h,$$

$$uu' + gh' = -c_f u^2/h, \qquad ww' + gh' = -c_f w^2/h,$$

$$vv' + 2qq' + \frac{q^2}{\eta}\,\eta' + \Big(g + \frac{q^2}{h}\Big)h' = \frac{\sigma q}{\eta}\,(u + w - 2v) - \frac{c_f}{h}\,(v^2 + q^2),$$

$$(vq)' = \frac{\sigma}{2\eta}\left((u-v)^2 + (w-v)^2 - (2+\varkappa)q^2\right) - \frac{2c_f}{h}\,vq$$

(the prime means the derivative with respect to x). After transformations, this system is converted to the form that is resolved with respect to the variables:

$$h' = \frac{G}{\Delta}, \qquad \xi' = \frac{c_f\xi}{h} - \frac{\sigma q}{u} - \frac{(u^2 - gh)\xi}{u^2 h}\,h', \qquad \zeta' = \frac{c_f\zeta}{h} - \frac{\sigma q}{w} - \frac{(w^2 - gh)\zeta}{w^2 h}\,h',$$

$$u' = -\frac{gh'}{u} - \frac{c_f u}{h}, \qquad w' = -\frac{gh'}{w} - \frac{c_f w}{h}, \qquad v' = \frac{2\sigma q - vY'}{\eta} + \frac{v}{\eta}\,(\xi' + \zeta') - \frac{v}{h}\,h', \tag{16}$$

$$q' = -\frac{q}{v}\,v' + \frac{\sigma}{2\eta v}\left((u-v)^2 + (w-v)^2 - (2+\varkappa)q^2\right) - \frac{2c_f}{h}\,q,$$

where

$$G = \frac{\sigma q}{(v^2 - 3q^2)v}\left((u-v)^2 + (w-v)^2 - (6+\varkappa)q^2 - (u+w-4v)v\right) - \Big(\frac{1}{u} + \frac{1}{w}\Big)\sigma q - Y' + \frac{c_f Y}{h},$$

$$\Delta = \frac{Y}{h} - \frac{g\xi}{u^2} - \frac{g\zeta}{w^2} - \frac{g\eta}{v^2 - 3q^2}.$$

The sign of the variable Δ determines whether the flow is subcritical ($\Delta < 0$) or supercritical ($\Delta > 0$).

2.2. Stationary Two-Layer and One-Layer Flows

In the course of evolution of the shear flow of a homogeneous fluid, the mixing layer may reach one of the side boundaries. In the stationary case, Eqs. (13) with allowance for corollaries (15) yield

$$(u\xi h)' = -\sigma q h, \qquad (v\eta h)' = \sigma q h, \qquad uu' + gh' = -c_f u^2/h,$$

$$vv' + gh' + \frac{1}{\eta h}\,(q^2\eta h)' = \frac{\sigma q}{\eta}\,(u - v) - \frac{c_f}{h}\,(v^2 + q^2),$$

$$(vq)' = \frac{\sigma}{2\eta}\left((u-v)^2 - (1+\varkappa)q^2\right) - \frac{2c_f}{h}\,vq.$$

These equations are also converted to the form resolved with respect to the derivatives; moreover, the differential equation for determining the thickness h coincides with the first equation of system (16), where the functions Δ and G should be replaced by Δ_1 and G_1 defined by the formulas

$$\Delta_1 = \frac{Y}{h} - \frac{g\xi}{u^2} - \frac{g\eta}{v^2 - 3q^2}, \qquad G_1 = \frac{c_f Y}{h} - Y' + \frac{\sigma q}{v}\,\frac{(u-v)^2 - (3+\varkappa)q^2 - (u-2v)v}{v^2 - 3q^2} - \frac{\sigma q}{u}.$$

At the last region of mixing layer development (one-layer flow region), the stationary solutions of model (14) are found from the equations

$$h' = \frac{G_2}{\Delta_2}, \qquad v' = -\frac{v}{h}\,h' - \frac{v}{Y}\,Y', \qquad q' = -\frac{q}{v}\,v' - \frac{\sigma\varkappa q^2}{2vY} - \frac{2c_f q}{h},$$

$$G_2 = \frac{c_f Y}{h} - Y' - \frac{\sigma\varkappa q^3}{(v^2-3q^2)v}, \qquad \Delta_2 = \frac{Y}{h} - \frac{gY}{v^2-3q^2}.$$

As in the situation considered above, the sign of Δ_j $(j = 1, 2)$ determines whether the flow is subcritical ($\Delta_j < 0$) or supercritical ($\Delta_j > 0$).

2.3. Initial Region of the Mixing Layer

The differential equations that describe a stationary mixing layer are derived above. To construct the solution, it is necessary to impose the conditions at the point of mixing layer formation, i.e., to find the asymptotics of the stationary solution (16) as $\eta \to 0$. Without loss of generality, we assume that $\eta = 0$ at $x = 0$, and the values of the functions at this point are marked by the zero subscript. Let the weakly shear layer parameters u_0, w_0, ξ_0, and ζ_0 and the total thickness of the layers h_0 be specified at the entrance of the mixing region; all values are positive and $\xi_0 + \zeta_0 = Y$. Let us assume that there are finite limits of the functions $v \to v_0 > 0$ and $q \to q_0 > 0$ as $x \to 0$ (or $\eta \to 0$) and find these values.

If the sought functions and their derivatives are bounded, we have $\eta' \to 2\sigma q_0/v_0$ and $\eta' \to (u_0+w_0-2v_0)\sigma/q_0$ by virtue of the second and sixth equations of system (16). Eliminating the limiting value of η' from these relations, we obtain

$$q_0^2 = (u_0 + w_0 - 2v_0)v_0/2. \tag{17}$$

The last equation of system (16) yields the relation

$$(u_0 - v_0)^2 + (w_0 - v_0)^2 - (2 + \varkappa)q_0^2 = 0. \tag{18}$$

From formulas (17) and (18), we obtain a quadratic equation for determining v_0:

$$v_0^2 - \frac{(3 + \varkappa/2)(u_0 + w_0)}{4 + \varkappa}v_0 + \frac{u_0^2 + w_0^2}{4 + \varkappa} = 0.$$

The conditions of existence of real roots of this equation were given in [18]. From physical considerations, we choose the value of v_0 satisfying the inequality $u_0 < v_0 < w_0$ (or $w_0 < v_0 < u_0$). This root is uniquely determined by means of varying the parameter $\varkappa$.

3. RESULTS OF NUMERICAL SIMULATIONS AND COMPARISONS WITH EXPERIMENTAL DATA

Results calculated by stationary and nonstationary equations of a layered horizontal shear fluid flow in an open channel are reported below. For convenience of comparisons with the experimental data [8], the calculations are performed for a straight channel 16 m long and 3 m wide. In all examples discussed below (except for the example illustrated in Fig. 3b), the free-stream parameters described in [8] are used: $u_0 = 0.118$ m/s, $w_0 = 0.238$ m/s, and $h_0 = 0.052$ m (case A). In what follows, we assume that $\xi_0 = \zeta_0 = 1.5$ m, $g = 9.8$ m/s^2, and $c_f = 0.003$ and use the following values of the empirical constants of model (10): $\sigma = 0.15$ and $\varkappa = 4$. It should be noted that the incoming flow in case A is subcritical.

3.1. Stationary Mixing Layer. Verification of the Model

The numerical implementation of the stationary solution of the problem of horizontal mixing layer development does not involve significant difficulties because it is described by a system of ordinary differential equations resolved with respect to the derivatives. With the use of the above-derived asymptotics as $\eta \to 0$, the solution can be constructed for both subcritical flow ($\Delta < 0$) and supercritical flow ($\Delta > 0$).

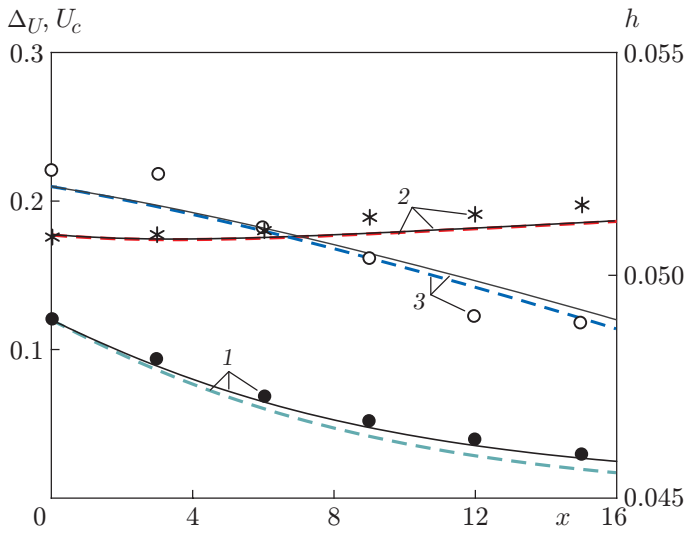

Fig. 2. Distributions of the velocity difference in the layers Δ_U (*1*), mean velocity U_c (*2*), and fluid layer thickness h (*3*) along the channel: the dashed curves show the solution of Eqs. (16), the solid curves show the calculated data [8], and the points are the experimental data [8].

Let the flows moving with the above-given velocities u_0 and w_0 merge in the cross section $x = 0$, where an intermediate mixing layer is formed. For the chosen values of the velocities and the parameter $\varkappa$, formulas (17) and (18) uniquely predict the values $v_0 \approx 0.171$ and $q_0 \approx 0.035$, which allows constructing the numerical solution of Eqs. (16) with specified values of the sought functions for $x = 0$. Let us use $\Delta_U = w - u$ and $U_c = (u + w)/2$ to denote the difference in the velocities in the weakly shear layers and their mean velocity, respectively.

Figure 2 shows the distributions of Δ_U, U_c, and h along the channel, which were obtained by solving Eqs. (16) (dashed curves). It follows from Fig. 2 that the theoretical and experimental data [8] are in good agreement. Similar correspondence for the velocity difference Δ_U and mean velocity U_c is also observed for other flow parameters described in [7, 8].

The following formula was proposed for determining the mixing layer width δ in [5, 6, 8]:

$$\frac{d\delta}{dx} = \alpha\lambda, \qquad \lambda = \frac{\Delta_U}{2U_c} \tag{19}$$

($\alpha = 0.1800 \pm 0.0015$). The same researchers also proposed to use a more general dependence including the dimensionless stabilization parameter S:

$$S = \frac{c_f \delta}{2h\lambda}. \tag{20}$$

It was noted that the mixing process is terminated if S exceeds the critical value $S_* \approx 0.12$, and it should be assumed that $\alpha = 0$ in Eq. (19).

Figure 3a shows the distribution of the mixing layer width η along the channel (curves *1*), which was predicted by model (16) (the flow parameters correspond to Fig. 2), and also the distribution of the width δ (curves *2*) found by solving Eq. (19) for $\alpha = 0.18$. The solution of Eqs. (16) is used for determining the right side of Eq. (19) because the values of Δ_U and U_c obtained by solving Eqs. (16) agree well with the experimental and numerical data [8]. Curves *3* show the distribution of the parameter S along the channel. The critical value $S_* = 0.12$ is reached at $x = x_*$. In the domain $x < x_*$, the values of the variables η and δ almost coincide, which serves as an additional confirmation of the correspondence of model (16) to the available results. The experimental points obtained in [8] for the mixing layer width lie higher than the predicted curves, which is caused by the complexity of precise determination of the layer boundaries. The mixing layer width determined by the proposed model may differ from the experimental data. Figure 3b shows similar predicted and experimental data for the incoming flow with the parameters $u_0 = 0.082$ m/s, $w_0 = 0.264$ m/s, and $h_0 = 0.059$ m (case D in [8]). It is seen that the agreement between the experimental and calculated values of the mixing layer width is improved by slightly increasing the flow depth h_0.

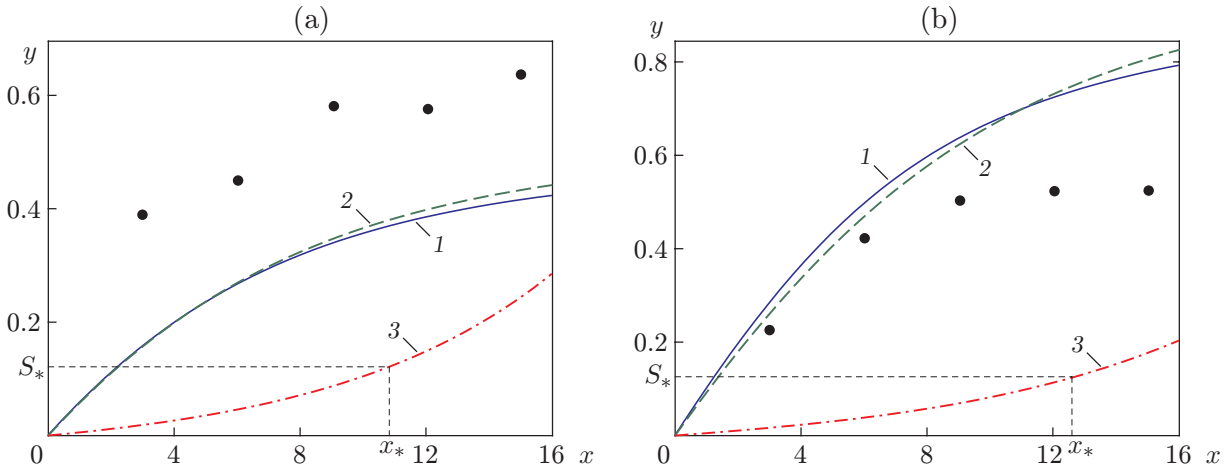

Fig. 3. Mixing layer width and dimensionless parameter of stabilization for the incoming flow with the parameters for case A (a) and case D (b): curve *1* shows the mixing layer width $\eta(x)$ predicted by model (16); curve *2* shows the mixing layer width $\delta(x)$ calculated by the empirical formula (19); curve *3* is the stabilization parameter S defined by formula (20); the points are the experimental data [8].

3.2. Reaching the Stationary Regime

The Nessyahu–Tadmor shock-capturing scheme of the predictor-corrector type [22] is applied for modeling nonstationary flows. This scheme was developed for solving conservative systems and has the second order of approximation. In nonstationary calculations by Eqs. (10), the values of h_0, ξ_0, ζ_0, u_0, w_0, v_0, and q_0 are used as the initial data at $t = 0$ in the entire computational domain and as the boundary conditions at $x = 0$. The solution of the stationary equations at the point $x = 16$ is imposed as the boundary condition on the right wall. It should be noted that a nonstationary regime of the flow with non-decaying oscillations may occur if other conditions at the channel exit are chosen in the case with $c_f > 0$ (e.g., von Neumann conditions). Discretization over the spatial variable x is performed on a uniform grid with the number of nodes $N = 400$. The time step is chosen automatically from the Courant condition.

Figure 4 shows the mixing layer boundaries $y = \xi$ and $y = \xi + \eta$) calculated at the time $t = 145$ (solid curves). The dashed curves show the solution of the nonstationary equations (16), which almost coincides with the nonstationary solution at a sufficiently large time. It is seen in Fig. 4 that the allowance for the bottom friction significantly affects the mixing process and the positions of the mixing layer boundaries. At $c_f = 0$ (see Fig. 4a), the mixing layer width increases and reaches the side walls of the channel at a sufficiently large distance from the entrance cross section. At $c_f = 0.003$ (see Fig. 4b), the mixing process is decelerated with distance from the entrance cross section, and the mixing layer width becomes stabilized. It should be noted that variations of the empirical parameters of mass transfer and energy dissipation in the admissible ranges $\sigma = 0.15$–0.20 and $\varkappa = 2$–4 does not exert any significant effect on the solution of Eqs. (10) or (16); in some particular cases, however, it ensures better agreement with the experimental data or results calculated by the two-dimensional equations (1). In particular, a decrease (increase) in the parameter $\varkappa$ leads to a minor increase (decrease) in the mixing layer width.

3.3. Comparison of Results Calculated by One-Dimensional and Two-Dimensional Models

The use of two-dimensional equations of the shallow water theory (1) offers a possibility of a detailed description of mixing and development of the Kelvin–Helmholtz instability in the case of confluence of flows moving with different velocities. However, detailed information on the flow structure, which requires the use of significant computational resources, is not always necessary. Averaged flow parameters can be rapidly determined by the proposed one-dimensional model of a three-layer flow (10) or (16).

Let us simulate the development of the Kelvin–Helmholtz instability at the interface between the layers within the framework of two-dimensional equations of the shallow water theory with allowance for friction (1)

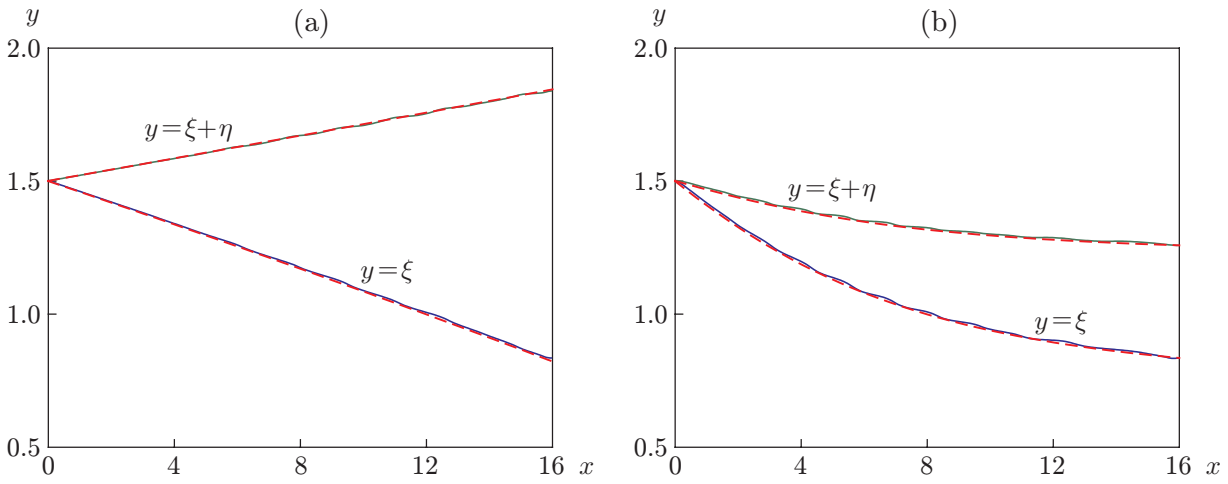

Fig. 4. Boundaries of the mixing layer obtained by solving the nonstationary equations (10) at $t = 145$ (solid curves) and stationary equations (16) (dashed curves) for $c_f = 0$ (a) and 0.003 (b).

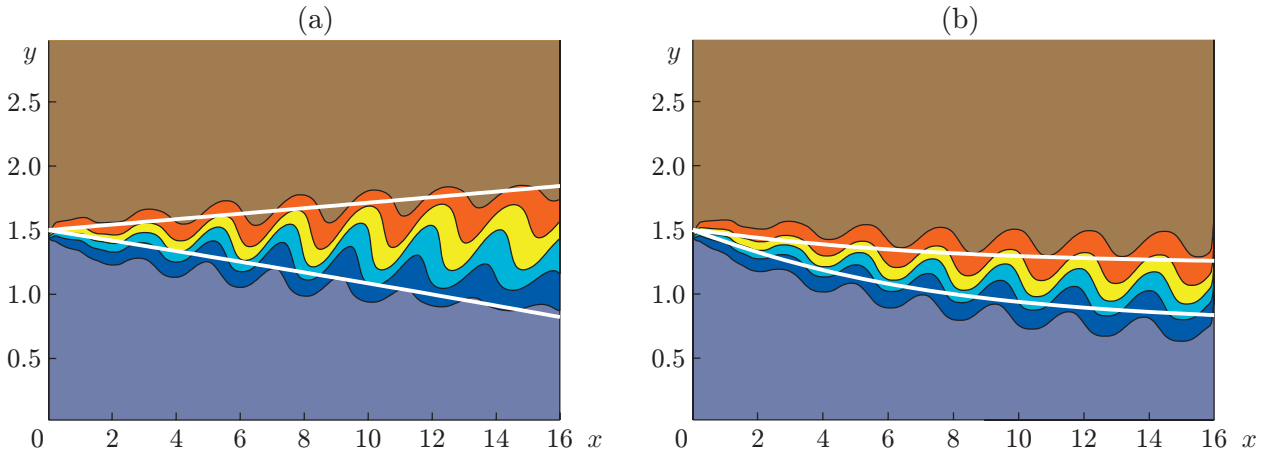

Fig. 5. Results of modeling the Kelvin–Helmholtz instability for $c_f = 0$ (a) and 0.003 (b); the thin curves show the levels of the function $c(t, x, y)$ with a step of 0.2 on the interval $[0, 1]$ at $t = 145$; the bold curves are the mixing layer boundaries calculated by model (16).

and compare these results with those calculated by the averaged model (16). For flow visualization, system (1) is supplemented with the equation

$$(ch)_t + (Uch)_x + (Vch)_y = 0 \tag{21}$$

for the function $c(t, x, y)$, which conserves along the trajectories and takes the values $c = 0$ and $c = 1$ in weakly shear layers moving with different velocities. In the course of flow evolution and mixing, the variable c takes intermediate values in the interval $[0, 1]$.

In the numerical solution of the nonstationary problem, we use a TVD scheme with a high order of approximation [22]. As the initial data at $t = 0$ for system (1), (21), we use the free-stream parameters $h = h_0$, $U = u_0$, and $c = 0$ at $0 \le y < Y/2$ or $U = w_0$ and $c = 1$ at $Y/2 < y \le Y$ and $V = 0$. These data are also used as the boundary conditions on the left at $x = 0$. The von Neumann condition is imposed on the right boundary. The side boundaries of the channel $y = 0$ and $y = Y$ are subjected to the condition $V = 0$. The calculations are performed on a uniform grid with the number of nodes $N_x = 400$ and $N_y = 75$ over the variables $x \in [0, 16]$ and $y \in [0, 3]$, respectively.

To generate vortices at the left boundary, a perturbation is inserted into the flow in the form of one-node shifting (increasing or decreasing) of the value $M_y = \text{round}\,(N_y/2 + \sin(\omega t))$ separating the flows moving with the velocities $U = u_0$ and $U = w_0$ at $x = 0$. The frequency ω affects the lengths of the waves formed with time. The results discussed below are obtained for $\omega = 0.5$.

Figure 5 shows the results of the two-dimensional calculation (variable c at $t = 145$) for the free-stream parameters corresponding to case A in [8] at $c_f = 0$ and 0.003. The bold lines show the mixing layer boundaries $y = \xi$ and $y = \xi + \eta$ obtained by solving the stationary equations (16) at $\sigma = 0.15$ and $\varkappa = 4$. It follows from Fig. 5 that bottom friction exerts a significant effect on the mixing process: the mixing layer is shifted to the flow region that has a smaller velocity in the inlet cross section. The mixing region predicted by the two-dimensional model is wider than the mixing region obtained by solving the one-dimensional equations. This is explained by the fact that the parameter determined in the one-dimensional layered model is the average position of the mixing layer boundary, whereas this position in the two-dimensional computation is perturbed owing to the presence of waves and vortices, as well as additional numerical dissipation.

CONCLUSIONS

A one-dimensional model of the formation and evolution of the mixing layer in shallow water flows with horizontal shear of velocity in open channels with allowance for bottom friction is proposed. The equations of motion are derived on the basis of a three-layer presentation of the flow within the framework of the shallow water theory with allowance for entrainment of the fluid from the weakly shear flow regions into the vortical interlayer. The velocity of fluid entrainment into the mixing layer is proportional to the velocity of "large eddies" generated in the vicinity of the interface between the layers. Particular attention is paid to studying the influence of bottom friction preventing the development of the mixing process and decelerating the enhancement of the mixing layer width with distance from the inlet cross section of the channel.

Stationary solutions of the three-layer flow equations are constructed and verified through comparisons with experimental data. The velocities in the weakly shear layers and the fluid layer thicknesses predicted by the proposed model are found to agree well with the results of [8]. The mixing layer widths determined theoretically and experimentally differ more significantly, which is caused, in particular, by certain "blurring" of the layer boundaries. Numerical solutions are constructed with the use of nonstationary homogeneous equations. In the case of constant boundary conditions, it is demonstrated that the solution reaches the steady state within a finite time. In the case with bottom friction, the mixing layer region becomes narrower, and this interlayer is shifted into the region with a slower flow. Comparisons with the results predicted by the two-dimensional equations of the shallow water theory show that the proposed simplified model provides a fairly accurate description of the main specific features of the flow and correct averaged parameters of the flow.

This work was supported by the Russian Foundation for Basic Research (Grant No. 16-01-00156).

REFERENCES

1. C. M. Ho and P. Huerre, "Perturbed Free Shear Layers," Annual Rev. Fluid Mech. **16**, 365–424 (1984).
2. W. S. J. Uijttewaal, "Hydrodynamics of Shallow Flows: Application to Rivers," J. Hydraul. Res. **52**, 157–172 (2014).
3. G. H. Jirka, "Large Scale Flow Structures and Mixing Processes in Shallow Flows," J. Hydraul. Res. **39**, 567–573 (2001).
4. B. L. Rhoads and A. N. Sukhodolov, "Lateral Momentum Flux and Spatial Evolution of Flow within a Confluence Mixing Interface," Water Resources Res. **44**, W08440 (2008).
5. V. Chu and S. Babarutsi, "Confinement and Bed-Friction Effects in Shallow Turbulent Mixing Layers," J. Hydraul. Eng. **114**, 1257–1274 (1988).
6. G. L. Brown and A. Roshko, "On Density Effects and Large Structure in Turbulent Mixing Layers," J. Fluid Mech. **64**, 775–816 (1974).
7. W. S. J. Uijttewaal and R. Booij, "Effects of Shallowness on the Development of Free-Surface Mixing Layers," Phys. Fluids **12**, 392–402 (2000).

8. R. Booij and J. Tukker, "Integral Model of Shallow Mixing Layer," J. Hydraul. Res. **39**, 169–179 (2001).
9. B. C. van Prooijen and W. S. J. Uijttewaal, "A Linear Approach for the Evolution of Coherent Structures in Shallow Mixing Layers," Phys. Fluids **14**, 4105–4114 (2002).
10. M. S. Ghidaoui and J. H. Liang, "Investigation of Shallow Mixing Layers by BGK Finite Volume Model," Int. J. Comput. Fluid Dyn. **22**, 523–537 (2008).
11. H. Liu, M. Y. Lam, and M. S. Ghidaoui, "A Numerical Study of Temporal Shallow Mixing Layers Using BGK-Based Schemes," Comput. Math. Appl. **59**, 2393–2402 (2010).
12. G. Kirkil, "Detached Eddy Simulation of Shallow Mixing Layer Development between Parallel Streams," J. Hydro-Environ. Res. **9**, 304–313 (2015).
13. D. J. Benney, "Some Properties of Long Nonlinear Waves," Studies Appl. Math. **52**, 45–50 (1973).
14. A. A. Chesnokov and V. Yu. Liapidevskii, "Wave Motion of an Ideal Fluid in a Narrow Open Channel," Prikl. Mekh. Tekh. Fiz. **50** (2), 61–71 (2009) [J. Appl. Mech. Tech. Phys. **50** (2), 220–228 (2009)].
15. A. A. Chesnokov V. Yu. Liapidevskii, "Shallow Water Equations for Shear Flows," Notes Numer. Fluid Mech. Multidisciplinary Design **115**, 165–179 (2001).
16. V. Yu. Liapidevskii and V. M. Tehukov, *Mathematical Models of Long Wave Propagation in an Inhomogeneous Fluid* (Izd. Sib. Otd. Ross. Akad. Nauk, Novosibirsk, 2000) [in Russian].
17. V. Yu. Liapidevskii and A. A. Chesnokov, "Mixing Layer under a Free Surface," Prikl. Mekh. Tekh. Fiz **55** (2), 127–140 (2014) [J. Appl. Mech. Tech. Phys. **55** (2), 299–310 (2014)].
18. V. Yu. Liapidevskii and A. A. Chesnokov, "Horizontal Mixing Layer in Shallow Water Flows," Izv. Ross. Akad. Nauk, Mekh. Zhidk. Gaza, No. 4, 91–107 (2016) [Fluid Dyn. **51** (4), 524–533 (2016)].
19. L. V. Ovsyannikov, "Two-Layer 'Shallow-Water' Models," Prikl. Mekh. Tekh. Fiz. **20** (2), 3–14 (1979) [J. Appl. Mech. Tech. Phys. **20** (2), 127–135 (2007)].
20. V. M. Teshukov, "Gas-Dynamic Analogy for Vortex Free-Boundary Flows," Prikl. Mekh. Tekh. Fiz. **48** (3), 8–15 (2007) [J. Appl. Mech. Tech. Phys. **48** (3), 303–309 (2007)].
21. S. L. Gavrilyuk, V. Yu. Liapidevskii, and A. A. Chesnokov, "Spilling Breakers in Shallow Water: Applications to Favre Waves and to the Shoaling and Breaking of Solitary Waves," J. Fluid Mech. **808**, 441–468 (2016).
22. H. Nessyahu and E. Tadmor, "Non-Oscillatory Central Differencing Schemes for Hyperbolic Conservation Laws," J. Comput. Phys. **87**, 408–463 (1990).